PROCEEDINGS OF SCIENCE

Atmospheric Neutrino Oscillations with the Super-Kamiokande detector

Magdalena Posiadala-Zezula
for the Super-Kamiokande Collaboration[a,*]

[a] *University of Warsaw,*
Krakowskie Przedmiescie 26/28, 00-927 Warsaw, Poland

E-mail: Magdalena.Posiadala@fuw.edu.pl

Analysis of the atmospheric neutrino data from all five run periods of Super-Kamiokande running with ultra-pure water, years 1996 - 2020, is presented. The fiducial volume region has been expanded from 22,5 kton to 27,2 kton, which allowed us to use also the events with reconstructed vertex at least 1 m from the nearest wall of the detector. Additional studies have been performed by adding information from T2K published binned data on muon neutrino disappearance and electron appearance. Over the range of parameters allowed at 90% confidence level, the normal mass ordering is favored based on the combined results from Super-Kamiokande and with T2K results.

41st International Conference on High Energy physics - ICHEP2022
6-13 July, 2022
Bologna, Italy

*Speaker

PoS(ICHEP2022)573

1. Introduction

Atmospheric neutrinos are created in the decays of particles produced in the interactions of primary cosmic rays with air nuclei. They are source of both neutrinos and antineutrinos with energies spanning from a few tens of MeV to more than 100 TeV. Produced neutrino flux is generated anywhere and it can be measured from all directions, which means that the pathlength that neutrinos need to travel before they reach Super-Kamiokande (Super-K) detector ranges from $\gtrsim$10 km up to 10,000 km.

2. The Super-Kamiokande detector and data set

Super-K is a cylindrical tank with 41.4 m height and 39.3 m in diameter. It is located in the mine at a depth of 2700 meters water equivalent in Gifu Prefecture, in Japan. The detector is filled with water and separated into inner detector (ID), used as primary target, and outer detector (OD), which is used as veto for external backgrounds. ID has 11,146 inward facing 50 cm photomultiplier tubes (PMTs) and 1,885 smaller PMTs that view OD. The more detailed descriptions and calibrations of the detector can be found in [2]. Detection principle is based on the Cherenkov radiation, emitted by the charged particles traveling through the detector's water. Some of the charged particles are generated while the neutrinos are propagating in the water. Moreover, there are many cosmic ray muons or low energy gammas from Rn or other radio isotopes. Emitted light is collected by the PMTs. We use PMTs timing information to reconstruct the interaction vertex. Particles are divided into two main categories based upon their Cherenkov ring pattern and opening angle. Rings from particles which produce electromagnetic showers, such as electrons and photons, tend to have fuzzy edges due to many overlapping rings from particles in the shower. They are labeled as *e*-like or showering. Muons and charged pions, which do not form showers, produce Cherenkov rings with crisp edges. Those rings are labeled as μ-like or non-showering. The reconstruction algorithm assigns the momenta to each reconstructed ring. Particles with higher momenta produce brighter Cherenkov rings. Since neutrino itself is not observed, the direction and energy variables which are used in the oscillation analysis are based on the information obtained from PMTs for the particles generated by the neutrino interaction with water or surrounding rocks.

Super-K has gone through seven run periods, since the start of the operation in 1996. The data with Super-K running with ultra-pure water are the subject of the analysis presented here and are divided into the periods from 1996 to 2001 (SK-I), from 2002 to 2005 (SK-II), from 2006 to 2008 (SK-III) and from 2008 to 2018 (SK-IV) and (2018-2020) SK-V. Photo-cathode coverage of the ID was equal to 40% except for the SK-II period with 20% coverage. Starting from SK-IV, new electronics was installed with which neutron tagging was possible to be measured even on with pure water. In total we used 6511,28 live-days of data collected among which 50% comes from SK-IV period.

3. Oscillation analysis

In the three neutrino flavor model of atmospheric neutrino oscillations are dominated by the effects of the mixing angle θ_{23} and mass splitting Δm^2_{32}. These parameters are responsible for the

main oscillation channel of $\nu_\mu \rightarrow \nu_\tau$. However, event by event identification of ν_τ at Super-K is difficult. The 3.5 GeV production threshold of the τ lepton and its short life time and prompt decay lead to high energy interactions with many visible particles (many rings in the event). They often mimic deep inelastic scattering (DIS) interactions of the ν_μ or ν_e neutrinos. Extraction of CC ν_τ interactions at Super-K is done using neural network (NN) algorithm and the first results from τ appearance at Super-K have been published in 2018 [3]. However, recently this analysis has been revisited and new results will be released soon [4].

The second, less dominant appearance channel to study is the one with oscillations of a type $\nu_\mu \rightarrow \nu_e$. Thanks to presence of matter effects we are here sensitive to neutrino mass ordering. Many atmospheric neutrinos travel large distances through the Earth before being detected at Super-K. Therefore, as particles undergoing weak interactions, these neutrinos are subject to scattering effects in matter. Any neutrino may scatter in the medium through the exchange of a Z-boson. However, since the Earth contains a large number of electrons, electron neutrinos may additionally interact with them via the $W^\pm$ boson while muon and tau neutrinos do not. On Fig.1 we present the oscillation probabilities for $\nu_\mu \rightarrow \nu_e$ (left) and $\bar{\nu}_\mu \rightarrow \bar{\nu}_e$ (right) as a function of energy and zenith angle assuming a normal mass ordering. Matter effects in the Earth produce the distortions in the neutrino figures between two and ten GeV, which are not present in the antineutrino plot. The height of this resonance is a function of both the matter density and the size of the parameter θ_{13}. Enhancements in the ν_e appearance probability occur primarily in angular regions corresponding to neutrino propagation across both the outer core and mantle regions (cosine zenith angle < -0.9) and propagation through the mantle and crust ($-0.9 <$ cosine zenith angle < -0.45). For an inverted ordering the matter effects appear in the antineutrino figure instead.

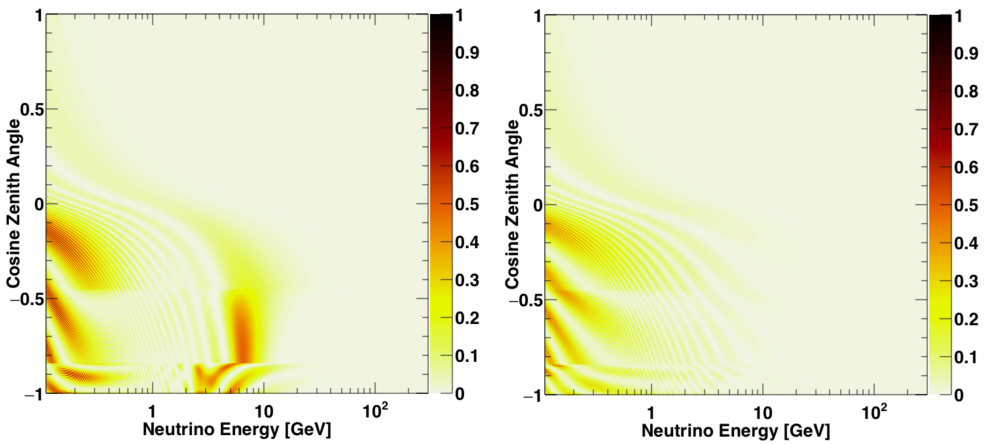

Figure 1: Oscillation probabilities for $\nu_\mu \rightarrow \nu_e$ (left) and $\bar{\nu}_\mu \rightarrow \bar{\nu}_e$ (right) as a function of energy and zenith angle assuming a normal mass ordering.

3.1 Improvements in the oscillation analysis

Several improvements have been made for the Super-K atmospheric oscillation analysis presented in this paper with respect to our last published results [1]. The most important ones are: expansion of fiducial volume to use events with reconstructed vertex present at least 1 m

from the nearest wall, this corresponds to 20% increase in statistics; usage of the SK-V data which corresponds to the 7% of the total available statistics; improvements in the neutrino - antineutrino selections by using information from the neutron tagging on hydrogen-(for SK-IV and SK-V) and finally the improvement of the classification for the multi-ring samples.

Expansion of Fiducial Volume. Major improvement done for this analysis is the fact the conventional fiducial volume (FV) was enlarged, from 22.4 kton to 27.2 kton. Also, particle identification performance was improved (in the expanded fiducial volume region). This was realized by improving the expected charge distribution in the analysis software. The last published results from atmospheric neutrino oscillations were using all the events which had reconstructed vertex located at least 2 m from the nearest wall (definition of the conventional FV region) [1]. The analysis presented in this paper uses also events with reconstructed vertex at least 1 m from the nearest wall. It allowed us to increase the data statistics by 20% thanks to the expanded FV region.

Improvements in the event selections for SK-IV and SK-V. Starting from SK-IV period, thanks to the electronic upgrade in 2008, we were able to use information on neutron tagging via hydrogen tagging. The 2.2 MeV signal from the de-excitation of deuterium after hydrogen neutron-capture is detectable. Despite the low energy of the signal, a tagging efficiency of 25% is achieved [5, 6]. Neutrinos produce on average fewer neutrons than antineutrinos. In addition to the usual cut on the number of electrons from muon decays for single-ring samples, a cut on the number of tagged neutrons (0 neutrons or >0 neutrons) is used to improve the neutrino antineutrino separation. This establishes new sample definitions for SK-IV and SK-V [6]. Another significant modification was the usage of machine learning techniques (a boosted decision tree, BDT, in this case) to improve the classification of multi-ring events into the four usual samples: CCν_e, CC$\bar{\nu}_e$, CC($\nu_\mu + \bar{\nu}_\mu$), and other (NC and CCν_τ). The implementation of this method increases the efficiency of the CCν_e-like sample, from 34.4% to 46.7% while maintaining a similar purity [6].

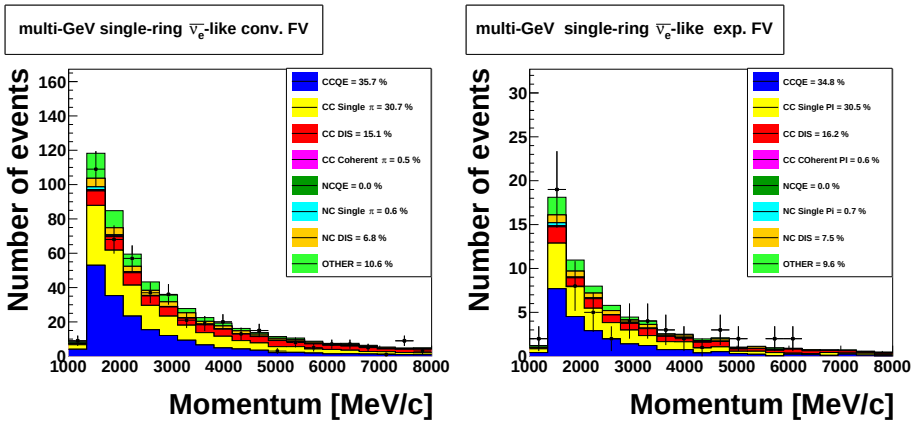

Figure 2: Momentum distributions for conventional FV (left) and expanded FV (right) regions for sample multi-GeV single-ring $\bar{\nu}_e$-like together with the expectations from the Monte Carlo for different reaction channels.

On Fig.2 we show the momentum distributions for conventional FV (left) and expanded FV (right) regions for multi-GeV single-ring $\bar{\nu}_e - like$ sample, for SK-IV period, together with the expectations from the Monte Carlo (MC) for different reaction channels. This sample is using neutron tagging information for selections. In both regions we can observe good agreement between data and MC. As expected, the most dominant reaction channel is CCQE $\bar{\nu}_e$- marked with the blue histogram. However, we still see large fraction of background interactions like CC single π interactions - yellow histograms or CC DIS - red histograms.

4. Results

Two main fits were performed, both using additional constraints on the value of $\sin 2\theta_{13} = 0.0220 \pm 0.0012$ [7] coming from the average of several reactor neutrino experiments. We used also measurements from the solar sector: $\sin 2\theta_{12} = 0.307$ and $\Delta m^2_{12} = 7.53x10^{-5}$ eV^2. Each fit was performed twice assuming two different mass orderings: normal and inverted. In the first fit we used all available atmospheric samples from Super-K. Fig. 3 represents constraints on neutrino oscillation parameters for this scenario.

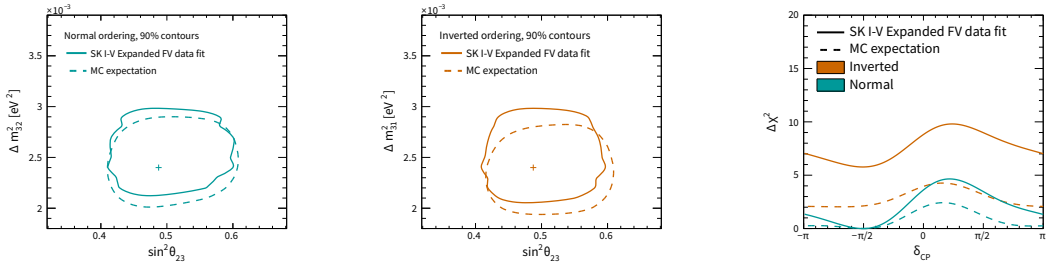

Figure 3: Constraints on neutrino oscillation parameters from the Super-K atmospheric neutrino data only. Results assuming normal ordering are presented with the blue line, while inverted ordering is shown with orange line. Solid lines represent the fit values using Super-K data while dashed lines show Monte Carlo expectations.

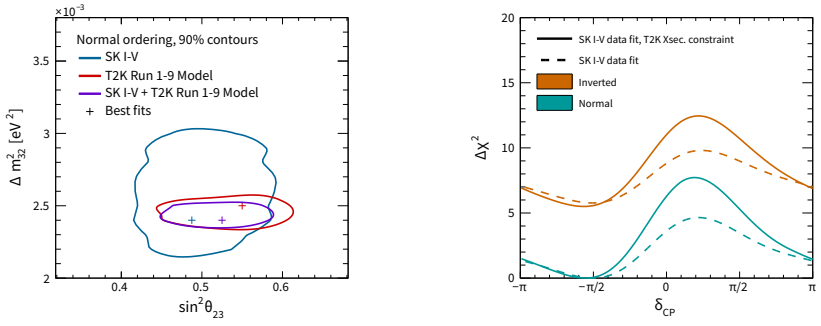

Figure 4: Constraints on neutrino oscillation contours from a combined fit of Super-K atmospheric neutrino data and a model of the T2K experiment.

In the second fit, apart from atmospheric Super-K measurements, additional data and systematic errors were introduced to accommodate the T2K results (referred later as T2K model) published in [8]. In this approach the addition of the T2K samples improves the constraint on the atmospheric mixing parameters due to T2K's more precise measurements. Fig. 4 represents constraints on neutrino oscillation parameters with Super-K and external T2K model.

In Tab.1 we present the best fit values from the analyses described above. In both fits the data slightly prefer the normal ordering over the inverted ordering with $\Delta\chi^2 = \chi^2_{IO} - \chi^2_{NO} = 5.8(8.9)$. for the Super-K only (Super-K + T2K model) results. The best fit value of δ_{CP} is 4.71 for both orderings (except from "Super-K + T2K model NO" case).

Fit:	χ^2	$\delta_{CP} \in (0, 2\pi)$	$\sin^2\theta_{23}$	Δm^2_{23}
Super-K NO	1000.42	4.71	0.49	$2.4 * 10^{-3}$ eV^2
Super-K IO	1006.19	4.71	0.49	$2.4 * 10^{-3}$ eV^2
Super-K + T2K model NO	1086.33	4.54	0.53	$2.4 * 10^{-3}$ eV^2
Super-K + T2K model IO	1095.25	4.71	0.53	$2.4 * 10^{-3}$ eV^2

Table 1: Best fit values from the Super-K only atmospheric neutrino data and with results obtained with the Super-K + T2K model.

5. Conclusions

Analysis of Super-Kamiokande atmospheric neutrino data for all pure water periods (SK-I to SK-V years 1996-2020) and with the expanded region, from 22.5 kton to 27.2 kton active volume of the detector, indicates a weak preference for the normal mass ordering. Fitting in conjunction with a model of the T2K experiment generally enhances these constraints and favors normal mass ordering.

References

[1] K.Abe, et al, (Super-Kamiokande Collaboration), Phys. Rev. D 97, 072011, (2018)

[2] S. Fukuda, et al. (Super-Kamiokande Collaboration), Nucl. Instr. Meth. A 501 418-462 (2003); K. Abe et al. (Super-Kamiokande Collaboration), Nucl. Instr. Meth. A 737, 253-272 (2014).

[3] S. Fukuda, et al. (Super-Kamiokande Collaboration), Phys.Rev.D 98, 052006 (2018)

[4] M. Mandal, et al. (Super-Kamiokande Collaboration), *Tau Neutrino Appearance in the Flux of Atmospheric Neutrinos at the Super-Kamiokande Experiment*, this proceedings.

[5] K.Abe, et al, (Super-Kamiokande Collaboration), arXiv:2209.08609v2 (2022)

[6] P. Fernandez Menendez, (Super-Kamiokande Collaboration), PoS ICRC2021 (2021)

[7] K. A. Olive et al. (Particle Data Group), Chin. Phys. C38, 090001 (2014).

[8] K. Abe, et al., (T2K Collaboration), Phys. Rev. D 103, 112008 (2021)